



# Sudden changes in nitrogen dioxide emissions over Greece due to lockdown after the outbreak of COVID-19

Maria-Elissavet Koukouli<sup>1</sup>, Ioanna Skoulidou<sup>1</sup>, Andreas Karavias<sup>2</sup>, Isaak Parcharidis<sup>2</sup>, Dimitris Balis<sup>1</sup>, Astrid Manders<sup>3</sup>, Arjo Segers<sup>3</sup>, Henk Eskes<sup>4</sup>, and Jos van Geffen<sup>4</sup>

<sup>1</sup>Laboratory of Atmospheric Physics, Aristotle University of Thessaloniki, Thessaloniki, Greece

<sup>2</sup>Department of Geography, Harokopio University, Athens, Greece

<sup>3</sup>TNO, Climate, Air and Sustainability, Utrecht, the Netherlands

<sup>4</sup>Royal Netherlands Meteorological Institute (KNMI), De Bilt, the Netherlands

**Correspondence:** Maria-Elissavet Koukouli (mariliza@auth.gr)

Received: 15 June 2020 – Discussion started: 27 July 2020

Revised: 29 December 2020 – Accepted: 31 December 2020 – Published: 9 February 2021

**Abstract.** The unprecedented order, in modern peaceful times, for a near-total lockdown of the Greek population as a means of protection against severe acute respiratory syndrome coronavirus 2, commonly known as COVID-19, has generated unintentional positive side-effects with respect to the country's air quality levels. Sentinel-5 Precursor/Tropospheric Monitoring Instrument (S5P/TROPOMI) monthly mean tropospheric nitrogen dioxide (NO<sub>2</sub>) observations show an average change of  $-34\%$  to  $+20\%$  and  $-39\%$  to  $-5\%$  with an average decrease of  $-15\%$  and  $-11\%$  for March and April 2020 respectively, compared with the previous year, over the six larger Greek metropolitan areas; this is mostly attributable to vehicular emission reductions. For the capital city of Athens, weekly analysis was statistically possible for the S5P/TROPOMI observations and revealed a marked decline in the NO<sub>2</sub> load of between  $-8\%$  and  $-43\%$  for 7 of the 8 weeks studied; this is in agreement with the equivalent Ozone Monitoring Instrument (OMI)/Aura observations as well as the ground-based estimates of a multi-axis differential optical absorption spectroscopy ground-based instrument. Chemical transport modelling of the NO<sub>2</sub> columns, provided by the Long Term Ozone Simulation European Operational Smog (LOTOS-EUROS) chemical transport model, shows that the magnitude of these reductions cannot solely be attributed to the difference in meteorological factors affecting NO<sub>2</sub> levels during March and April 2020 and the equivalent time periods of the previous year. Taking this factor into account, the resulting decline was estimated to range between  $\sim -25\%$  and  $-65\%$  for 5 of the 8 weeks studied,

with the remaining 3 weeks showing a positive average of  $\sim 10\%$ ; this positive average was postulated to be due to the uncertainty of the methodology, which is based on differences. As a result this analysis, we conclude that the effect of the COVID-19 lockdown and the restriction of transport emissions over Greece is  $\sim -10\%$ . As transport is the second largest sector (after industry) affecting Greece's air quality, this occasion may well help policymakers to enforce more targeted measures to aid Greece in further reducing emissions according to international air quality standards.

## 1 Introduction

In this work, we aim to quantify the decline in tropospheric nitrogen dioxide (NO<sub>2</sub>) levels over Greece during the ongoing severe acute respiratory syndrome coronavirus 2 (COVID-19) pandemic, as sensed by the spaceborne S5P/TROPOMI (hereafter referred to as TROPOMI) instrument. By comparing the relative levels for the months of March and April for the years 2020 and 2019, while properly accounting for the differences in meteorology using the simulations of a chemical transport model (CTM), we quantify the improvement in local and regional air quality due to the reduced nitrogen oxides (NO<sub>x</sub>) emissions.

In the following sections, we provide basic information on tropospheric NO<sub>x</sub>, focus on current knowledge of the nominal NO<sub>x</sub> emissions over Greece, present a brief overview of the capabilities of current and past satellite instruments

with respect to sensing abrupt atmospheric content changes, and provide the dates when the different lockdown measures were enforced nationwide in Greece.

### 1.1 Nitrogen oxides in the troposphere

Nitrogen dioxide (NO<sub>2</sub>) and nitrogen oxide (NO), referred to more commonly as nitrogen oxides (NO<sub>x</sub>), are important trace gases in the Earth's troposphere. NO<sub>x</sub> are emitted as a result of both anthropogenic activities, such as fossil fuel combustion and biomass burning, and natural processes, such as microbiological processes in soils, wildfires and lightning. In the presence of sunlight, the photochemical cycle of tropospheric ozone (O<sub>3</sub>) converts NO into NO<sub>2</sub> on a timescale of minutes; thus, NO<sub>2</sub> is considered a robust measure for concentrations of nitrogen oxides (Jacob, 1999). For typical levels of the OH radical, the lifetime of NO<sub>x</sub> in the lower troposphere is less than a day – normally a few hours depending on the season and the rates of the photochemical reactions (e.g. Beirle et al., 2011; Mijling and van der A, 2012). As a result, it is well accepted that NO<sub>2</sub> fluxes will remain relatively close to their source which, first of all, makes it possible for NO<sub>x</sub> emissions to be well detected from space (e.g. Stavrou et al., 2008; Lamsal et al., 2010; van der A et al., 2008) but also precludes any transboundary pollution effects which might otherwise hinder this study.

In the troposphere, NO<sub>2</sub> plays a key role in air quality issues, as it directly affects human health (WHO, 2016). In the European Union, the evidence of NO<sub>2</sub> health effects has led to the establishment of air quality standards for the protection of human health. Limit values for NO<sub>2</sub> are set at 200 µg m<sup>-3</sup> for 1 h average concentrations (with 18 exceedances permitted per year) and at 40 µg m<sup>-3</sup> for annual average concentrations (European Council Directive 2008/50/EC, <https://eur-lex.europa.eu/eli/dir/2008/50/oj>, last access: 9 February 2021). Concentrations above the annual limit value for NO<sub>2</sub> are still widely registered across Europe, even if concentrations and exposures continue to decrease (EEA, 2019a). In Greece in particular, the annual average standard of 40 µg m<sup>-3</sup> was not exceeded between 2007 and 2017 considering all in situ stations; however, the traffic stations of Athens and Thessaloniki show annual levels of up to 45 µg m<sup>-3</sup> for 2015 to 2017. Hence, it follows logically that closely monitoring abrupt changes in NO<sub>x</sub> emissions for diverse locations plays a key role in shaping future environmental policies and directives.

### 1.2 Nitrogen dioxide emissions over Greece

According to the EEA Report No. 8/2019 (EEA, 2019b), updated by the EU 2019 Environmental Implementation Review for Greece (EU, 2019), the country's NO<sub>x</sub> emissions by sector originate from road transport, industry (which mainly covers the energy production and distribution sector), non-road transport, household and agriculture. The relative per-

centages for NO<sub>x</sub> air emissions, separated by sector, as extracted from the Air Emission Account 2017 report from the Hellenic Statistical Authority (HAS, 2017), are as follows: industry, 48 %; transport, 22 %; energy supply, 18 %; manufacturing, 6 %; central heating, 4 %; agriculture, 1 %; and others, 1 %. Based on the European Environment Agency (EEA) European Pollutant Release and Transfer Register, 77 % of the reported industrial NO<sub>x</sub> / NO<sub>2</sub> emissions over Greece came from thermal power stations and other combustion installations. The monthly energy balance reports, composed by the Independent Power Transmission Operator of the Hellenic Electricity Transmission System (IPTO, 2020), show that the total energy requested for March 2020 (4.152 GWh) was -2.1 % lower than 2019 (4.224 GWh), whereas for April 2020 (3.527 GWh), it was -9.8 % lower than 2019 (3.527 GWh). These reductions are quite typical of the seasonality of the energy consumption in Greece which peaks in December and January, due to heating needs, and in July and August, due to cooling needs, with seasonal lows in spring (April and May) and autumn (October and November). Furthermore, Fameli and Asimakopoulou (2015) reported that the annual mean NO<sub>x</sub> emissions for Greece for 2006 to 2012 can be attributed as follows, in order of relevance: industry, 45 ± 3 %; road transport, 35 ± 8 %; shipping, 11 ± 3 %; non-road transport, 10 ± 4 %; central heating, 5 ± 2 %; and agriculture and aviation, an average of around 1 ± respectively. If we assume that 2019 and 2020 were not exceptional in their temperature levels for the spring months, it follows that changes in central heating emissions will not be a significant part of the emission changes observed.

### 1.3 Sensing abrupt emission changes from space-borne sensors

Abrupt emission changes have already been reported using space-borne observations for a number of recent local and continental circumstances. Castellanos and Boersma (2012) reported significant reductions in nitrogen oxides over Europe driven by environmental policy and the economic recession based on Ozone Monitoring Instrument (OMI)/Aura observations between 2004 and 2010. Vrekoussis et al. (2013) and Zyrichidou et al. (2019) reported strong correlations between pollutant levels and economic indicators, showing that the 2008 economic recession resulted in proportionally lower levels of pollutants over large parts of Greece. For 2008 to 2015, the latter study surprisingly found that while the wintertime tropospheric NO<sub>2</sub> trends were negative, significant positive formaldehyde trends were observed from space, which were shown to be due to increased usage of affordable indoor heating methods (e.g. fireplaces and wood stoves). Space-sensed reductions in emissions on a shorter timescale have also been attributed to strict measures enforced for benign reasons. Using OMI/Aura and CTM results, Mijling et al. (2009) calculated reductions in NO<sub>2</sub> concentrations of ap-

proximately 60 % above Beijing during the 2008 Olympic and Paralympic games. Ding et al. (2015) showed a  $\sim 30$  % decrease in OMI/Aura columns, which was translated into a  $\sim 25$  % in actual emission levels during the Nanjing 2014 Youth Olympic Games.

Numerous first reports suggesting improved air quality after the COVID-19 lockdown was enforced have already been detailed by major media outlets. Here, we note the findings of Liu et al. (2020), who (based on both OMI/Aura and TROPOMI) reported a 48 % drop in tropospheric NO<sub>2</sub> in China from the 20 d averaged before the 2020 Lunar New Year to the 20 d after; this decrease is 20 % larger than that from recent years, and the authors related the strengthened NO<sub>2</sub> decline to the date of each Chinese provincial lockdown. Similar levels of tropospheric NO<sub>2</sub> decrease over different Chinese provinces have been reported by Ding et al. (2020) and Miyazaki et al. (2020). Bauwens et al. (2020), using the same sensors, also reported an average NO<sub>2</sub> column drop over all Chinese cities of  $-40$  % relative to the same period in 2019, whereas the decreases in western Europe and the US were found to range between  $-20$  % and  $-8$  %. Goldberg et al. (2020) analysed TROPOMI observations around large US cities, focusing on the effect of meteorological factors, and reported that meteorological variations between 2019 and 2020 can cause columnar NO<sub>2</sub> differences of  $\sim 15$  % over monthly timescales. Compensating for meteorology, they then calculated a decrease in NO<sub>2</sub> levels between 9.2 % and 43.4 % among 20 cities in North America, with a median of 21.6 %. Cersosimo et al. (2020) re-gridded the TROPOMI observations down to the  $1 \times 1$  km level and found that the reductions measured by air quality in situ measurements in the Po Valley, Italy, were very well reproduced by the satellite observations, whereas comparisons over less polluted regions in the south of Italy provide mixed results, which may also be attributed to the lower space-sensed levels. Virghileanu et al. (2020) analysed the lockdown effect on Europe-wide pollution and reported correlations with in situ observations ranging between 0.5 and 0.75 while also demonstrating the usefulness of such high spatial resolution satellite observations when used in tandem with other economic factors.

#### 1.4 The COVID-19 situation over Greece

A short review on the COVID-19 situation over Greece is given here, mainly focusing on providing the dates in March 2020 of the successive restrictive measures that were enforced nationwide and affected NO<sub>x</sub> emissions. The country's General Secretariat for Civil Protection reacted quickly to the emerging situation in neighbouring Italy, and long before the first casualties were reported, major festivities for the carnival season (planned for the 28 February to the 2 March) were cancelled; this was followed by the cancellation of all other cultural and sporting activities on 8 March. On the 11 March, all levels of education were suspended and

a first wave of workplace closures begun; this culminated on Monday 16 March when all restaurants, coffee shops with seating facilities, and the general food (apart from supermarkets) and hospitality industries were shut down. During the following 2 d, all remaining retail activity was suspended apart from pharmacies. On Monday 16 March, restrictions on the size of public gatherings were announced, and the public transport sector (buses, trams, underground and trains) started to reduce their capacity. On Monday 23 March, full restrictions on the population's movements were imposed with strict stay-at-home mandates (with exceptions for essential working personnel), including all religion-related congregations, with a complete and comprehensive restriction around the Greek Orthodox Easter holiday on 19 April. The country remained in full lockdown until 4 May. We should note here that most industrial activities maintained normal operations, albeit with a skeleton crew, which might account for some of the higher load observed around the city of Athens where most of these activities are located.

## 2 Materials and methods

In this section, we introduce the TROPOMI tropospheric NO<sub>2</sub> observations, the Long Term Ozone Simulation European Operational Smog (LOTOS-EUROS) CTM simulations and the proposed methodology to account for the different meteorological conditions between the nominal period of March–April 2019 and the disrupted one of March–April 2020.

### 2.1 TROPOMI NO<sub>2</sub> observations

The recently launched TROPOMI instrument on the Sentinel-5 Precursor (S5P) mission (Veefkind et al., 2012) has been providing global atmospheric observations since early 2018. Its very high spatial resolution of  $3.5 \times 7$  km<sup>2</sup>, upgraded to  $3.5 \times 5.5$  km<sup>2</sup> in August 2019, and improved signal-to-noise ratio compared with previous space-borne instruments, permits the detection of tropospheric pollution from small-scale emission sources as well as the estimation of very localized emissions from anthropogenic activities, such as industrial point sources, and regional fires. Lorente et al. (2019) have already reported updated emissions over the Paris metropolitan area using TROPOMI observations, and Ialognio et al. (2020) have assessed the capabilities of this instrument in evaluating city-wide air quality levels compared with the more traditional ground-based and in situ NO<sub>2</sub> monitoring methods.

In this work, we use the publicly available TROPOMI offline v1.2 and v1.3 tropospheric NO<sub>2</sub> data for March–April 2019 and for March–April 2020, accessed via the Copernicus Open Access Hub. The algorithm producing these data is described by van Geffen et al. (2019) and is based on the approach used for processing OMI/Aura NO<sub>2</sub> data within

DOMINO (Dutch OMI NO<sub>2</sub>) and the FP7 Quality Assurance for Essential Climate Variables projects (Boersma et al., 2011, 2018). Routine validation is being carried out by the Validation Data Analysis Facility, who also provide the quarterly validation report of the Copernicus Sentinel-5 Precursor Operational Data Products. The S5P tropospheric NO<sub>2</sub> columns are routinely compared to ground-based column data at 19 ground-based multi-axis differential optical absorption spectroscopy (MAXDOAS) stations. The latest report describes a negative bias of typically −22 % to −37 % for clean and slightly polluted conditions, reaching values of −51 % over highly polluted areas (ROCVR #08, 2020). Furthermore, within ROCVR #08, the case of Athens was used as an example of the lockdown effects on NO<sub>2</sub> observations from both ground and space. It is shown that both the Athens MAXDOAS instrument (operated by the Institute of Environmental Physics, University of Bremen) and the S5P observations evidence a significant drop in NO<sub>2</sub> levels between 3 and 13 March, which is in line with the first nation-wide measures on 10 March 2020, with further restrictions on later days (e.g. closure of business, ban on non-essential movement; see <https://www.bloomberg.com/news/articles/2020-04-17/humbled-greeks-show-the-world-how-to-handle-the-virus-outbreak>, last access: 3 February 2021). NO<sub>2</sub> columns over Athens remained consistently low for weeks afterwards, and the MAXDOAS instrument performed very well overall, with a mean difference to the TROPOMI observations of  $1.40 \pm 3.50 \times 10^{15}$  molec. cm<sup>−2</sup> (median of  $0.25 \times 10^{15}$  molec. cm<sup>−2</sup>) for the 385 coincident days of observations between 1 May 2018 and 28 November 2020 (<https://mpc-vdaf-server.tropomi.eu/no2/no2-offl-maxdoas/athens>, last access: 3 February 2021). We should note at this point that as the main findings in this work refer to relative differences between different time periods, absolute differences to standard instruments do not affect our findings because the stability of the TROPOMI datasets is assured.

For the purposes of this work, orbital files over Greece, between 19 and 30° E and 34 and 42° N, were gridded onto a  $0.10 \times 0.05^\circ$  grid for different temporal scenarios. The data have been filtered, as recommended, using the quality flag indicator  $\geq 75$  which assures that the data under this flag are restricted to cloud-free (cloud radiance fraction  $< 0.5$ ) and snow- and ice-free observations. An example figure is presented in Sect. 3.1 (Fig. 1) where the major NO<sub>x</sub>-emitting sectors around Greece are prominent, including the capital city Athens and the second largest city Thessaloniki (in the north), emissions by one of the two largest thermal power plants in Ptolemaida (also in the north) and an important thermal power plant in the Republic of North Macedonia (near the Greek border), where such transborder pollution transport is often visible. The domain also includes major emissions from known locations on the Turkish Asia Minor coast, originating from both cities and major power plant activities, as well as the major shipping track that emerges from

the Bosphorus Strait in Istanbul moving south-west towards Athens before turning westward towards the Mediterranean Sea.

## 2.2 LOTOS-EUROS CTM simulations

The open-source LOTOS–EUROS v2.2.001 chemical transport model is used for the purposes of this study to simulate NO<sub>2</sub> columns over the Greek domain for March and April for 2019 and 2020. The CTM model (<https://lotos-euros.tno.nl/>, last access: 3 February 2021) is originally aimed at air pollution studies and simulates gases (e.g. O<sub>3</sub>, NO<sub>x</sub> and SO<sub>2</sub>) as well as aerosols (e.g. sulfate, nitrate, PM<sub>10</sub> and PM<sub>2.5</sub>) in the troposphere. The gas-phase chemistry of the model is a modified version of the Carbon Bond Mechanism IV (CBM-IV; Gery et al., 1989), and the ISORROPIA II module (Fountoukis and Nenes, 2007) is used for the aerosol chemistry. Detailed information on the model and its activity can be found in Manders et al. (2017). LOTOS-EUROS is the national air quality model for the Netherlands (Vlemmix et al., 2015) and has been used for specific studies as well to investigate NO<sub>2</sub> values (Timmermans et al., 2011; Curier et al., 2012, 2014). LOTOS-EUROS also participates in the operational Copernicus Atmosphere Monitoring Service (CAMS), comprising one of the seven CTMs that provide the official CAMS ensemble air quality forecasting service, and its capabilities have been demonstrated during the European Monitoring Atmospheric Composition and Climate (MACC) project and the MACC-II (Monitoring Atmospheric Composition and Climate: Interim Implementation) project (Marécal et al., 2015). Vlemmix et al. (2015) compared LOTOS-EUROS NO<sub>2</sub> tropospheric columns with MAXDOAS measurements and found a good agreement between the two datasets, with a correlation coefficient between the daily averaged columns of 0.72. Schaap et al. (2013) compared the LOTOS-EUROS NO<sub>2</sub> simulations with OMI/Aura retrievals and also showed that the model captures the NO<sub>2</sub> spatial distribution satisfactorily and is able to explain 91 % of the OMI signal variation across Europe, while the systematic difference was attributed to the summer period.

In this work, LOTOS-EUROS NO<sub>2</sub> simulations over Greece already presented and discussed thoroughly in Skoulidou et al. (2020) are used. The model uses offline meteorology extracted from the Operational Forecast data from the European Centre for Medium-Range Weather Forecasts (ECMWF). These meteorological model level fields cover parameters such as temperature, boundary layer height, specific humidity, wind components, half-level pressures, cloud cover, cloud liquid and ice water content, rain and snow water content, total cloud cover, convective and large-scale precipitation and wind components at 10 m. In addition, surface fields that include orography, soil type, land–sea mask, sea surface and soil temperature, dew point temperature at 2 m, surface latent and sensible heat fluxes and surface solar downward radiation, among others, are also included. The

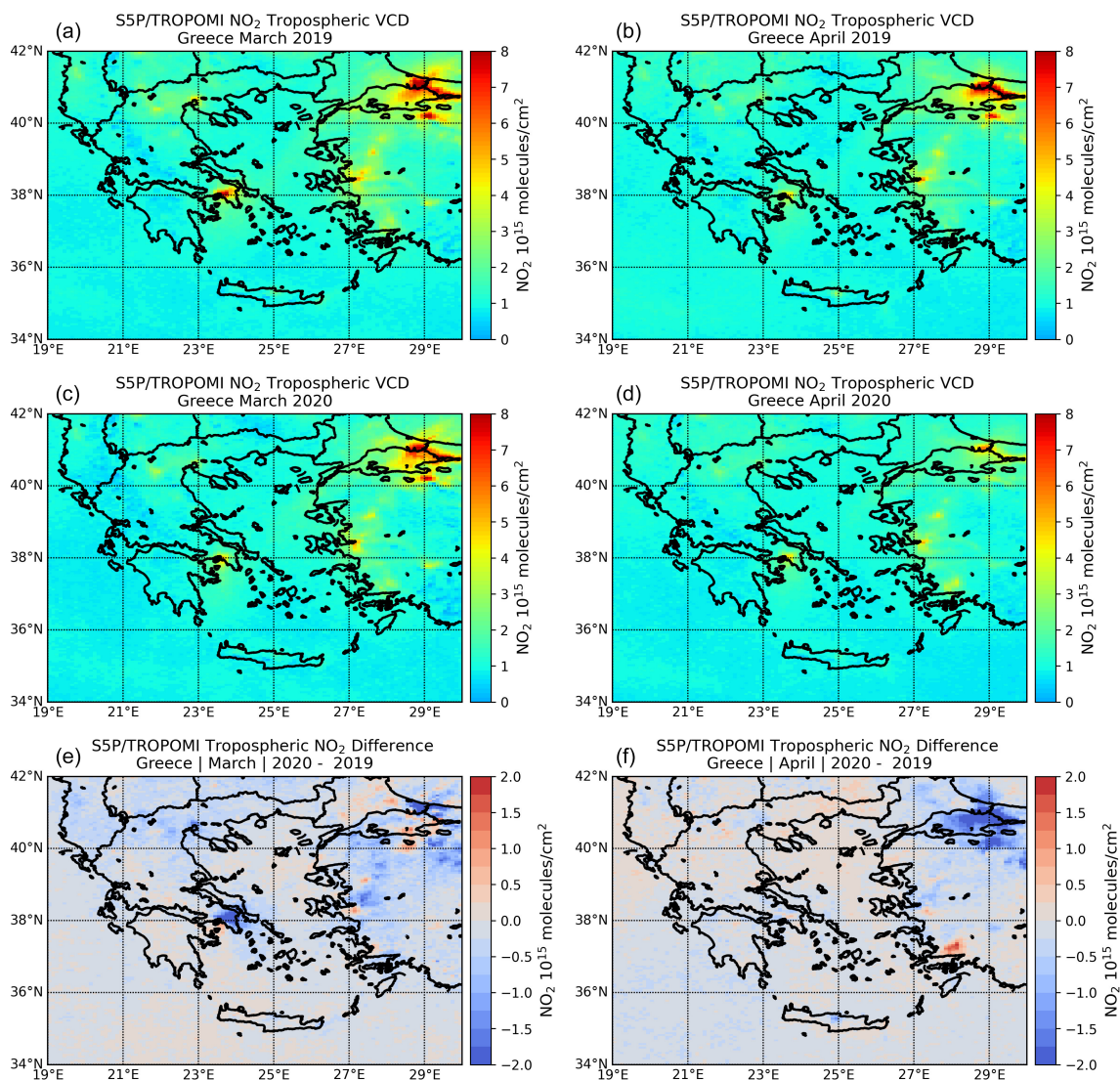


**Figure 1.** Monthly mean TROPOMI tropospheric  $\text{NO}_2$  columns (in  $10^{15} \text{ molec. cm}^{-2}$ ) for March (a, c, e) and April (b, d, f) for 2019 (a, b) and 2020 (c, d) as well as their absolute differences (e, f).

different level type fields are obtained at a 3 h temporal resolution, whereas the surface fields are imported at a 1 h resolution. The horizontal resolution of the meteorological input fields is  $7 \text{ km} \times 7 \text{ km}$ . In the vertical domain, the model distinguishes 10 levels that extend from the surface to about 175 hPa. The height of these levels refers to the levels of the ECMWF meteorological input data that are further used to drive the model runs. The initial and boundary conditions are constrained from a coarser run of LOTOS-EUROS that is performed over the larger European domain ( $15^\circ \text{ W} - 45^\circ \text{ E}$  and  $30 - 60^\circ \text{ N}$ ) with a resolution of  $0.25^\circ \times 0.25^\circ$ , as discussed in Skoulidou et al. (2020). The anthropogenic emissions are provided by the CAMS-REG (CAMS Regional Emissions) inventory for Europe for the year 2015 with a horizontal resolution of  $0.1^\circ \times 0.05^\circ$  (Kuenen et al., 2014).

The LOTOS-EUROS  $\text{NO}_2$  simulations over Greece reproduce the spatial variability of the TROPOMI  $\text{NO}_2$  columns over Greece very well, capturing the locations of low and high  $\text{NO}_2$  columns (see their Figs. 11 and 12 for the summer and winter period respectively). The spatial correlation between the simulations over Athens (Thessaloniki) and the TROPOMI observations is 0.95 (0.82) in summer and 0.82 (0.66) in winter, with a bias of  $\pm 18\%$  ( $+4\%$  to  $-27\%$ ). Furthermore, comparisons to MAXDOAS systems located in both cities have shown that LOTOS-EUROS simulates the diurnal variability of the  $\text{NO}_2$  very well, with biases between 0% and 30% depending on the season for the overpass time of TROPOMI (around 12:00 UTC), which is in quite good agreement with what was found in Vlemmix et al. (2015) and Blechschmidt et al. (2020).

### 2.3 Comparative methodology

While it would make sense to simply compare the NO<sub>2</sub> levels over Greece for the two periods, assuming that the emission sources have not changed dramatically between 2019 and 2020, one should not discard the effects that various meteorological parameters have on NO<sub>2</sub> levels (Goldberg et al., 2020). Meteorological conditions, such as wind speed, temperature inversions and the depth of the boundary layer, often play pivotal roles in local air quality levels (Jacob and Winner, 2009). The ambient levels of secondary NO<sub>2</sub> pollution are determined through the accumulation or dispersion of pollutants, low or high solar irradiances, regional transport of clear or polluted air and atmospheric chemistry for the formation of secondary species, in this case via the chemical coupling of NO<sub>x</sub> with O<sub>3</sub> (e.g. Seo et al., 2017).

To ensure that the observed decrease in NO<sub>2</sub> levels was not due to diverse meteorological conditions between one year and the next, relative differences in NO<sub>2</sub> columns provided by the LOTOS-EUROS model are calculated, and their average magnitude is set as the expected contribution from the different meteorology. This forms a standard level above which we expect COVID-19-related reductions, i.e. emission-related reductions. The premise of this thinking is as follows: differences in the satellite observations will contain the intertwined effect of differences in meteorology on concentrations and of differences in emissions. For the model, we keep the emissions constant for the two periods but use the meteorology of 2019 and 2020 so that we can isolate the impact of meteorology on concentrations. We cannot of course exclude the possibility that the LOTOS-EUROS model has biases in the resulting NO<sub>2</sub> column depending on the meteorological conditions. In Skoulidou et al. (2020), differences in night-time surface concentrations between in situ observations and model simulations were found and were attributed to modelling uncertainties in mixing under stable conditions. Within the methodology followed in this work, we expect any possible biases to cancel out in the difference fields calculated.

At this point, we should stress that the satellite observations are more often than not gap-ridden, as all but nearly clear-skies remain in the suggested screening. Springtime months are rainy months, even for typically sunny Greece, which means that a one-to-one comparison of the satellite observations for the two periods, even on a weekly basis, is usually impossible. For example, during our analysis it was found that the last week of March in 2020, the first week of full lockdown, was fully cloudy for northern Greece, even though the equivalent week in March 2019 was entirely sunny. As a result, weekly comparisons were only possible for the major NO<sub>2</sub> hotspot over Greece, the city of Athens, whereas the rest of the domain was examined on a monthly basis.

In technical terms, the LOTOS-EUROS simulations were performed on the entire timeline as discussed in Sect. 2.2

but were restricted, on a daily basis, to the TROPOMI pixels that actually provided an observation when performing the temporal averaging and producing the comparative plots. Even though a direct comparison of the CTM results to the satellite data is not the focus of this paper, we imposed this filter to make sure that the same days with the same meteorological conditions were viewed by both methods. Furthermore, as discussed in Eskes and Boersma (2003), so as to properly compare the modelled and measured columnar data, we applied the TROPOMI averaging kernels (AKs) to the modelled profiles before extracting the CTM columns. The LOTOS-EUROS CTM includes a module that imports the TROPOMI NO<sub>2</sub> orbital files in a predefined format, performs all the necessary filtering, regridding and averaging of the datasets, and executes the AK convolution of the nearest (in time) observation to the CTM NO<sub>2</sub> simulated profile before outputting the profile and columnar information on the predefined spatio-temporal grid.

## 3 Results

In the following section, we first show the effect on monthly NO<sub>2</sub> levels over the entire domain, the six Greek cities with the largest number of inhabitants, and we then present a more in depth analysis, on a weekly basis, for the city of Athens, also examining the long-term variability of tropospheric NO<sub>2</sub> levels over the capital city using 15 years of space-borne observations by the Ozone Monitoring Instrument (OMI/Aura) as well as the air quality in situ measurements of the Greek Ministry Environment and Energy network, reporting to the European Environment Agency.

### 3.1 Lockdown effects on monthly NO<sub>2</sub> levels

In Fig. 1, the monthly mean tropospheric NO<sub>2</sub> levels over Greece, the northern neighbouring countries, the Aegean Sea, and the coast of Turkey and Istanbul area, are shown for 2019 (Fig. 1a, b), 2020 (Fig. 1c, d), and their absolute difference (Fig. 1e, f), for the month of March (Fig. 1a, c, e) and the month of April (Fig. 1b, d, f). Even though the hotspots appear strong for year 2019, with discrete shipping tracks and ground-tracks over Turkey being clearly displayed, the different meteorological conditions between March and April obviously affect both the location of the maxima and the absolute level of the maxima. As Greece gradually entered full lockdown mode within the first 3 weeks of March, whereas Turkey imposed intermittent movement restrictions from the beginning of April onwards, the NO<sub>2</sub> hotspot around the megacity of Istanbul and the Bosphorus Strait is still pronounced in March 2020 (Fig. 1c), whereas most of the smaller urban emission points are missing in Greece, and Athens is shown to be in sharp decline. In April 2020, the Turkish hotspots are also reduced in magnitude, as expected.

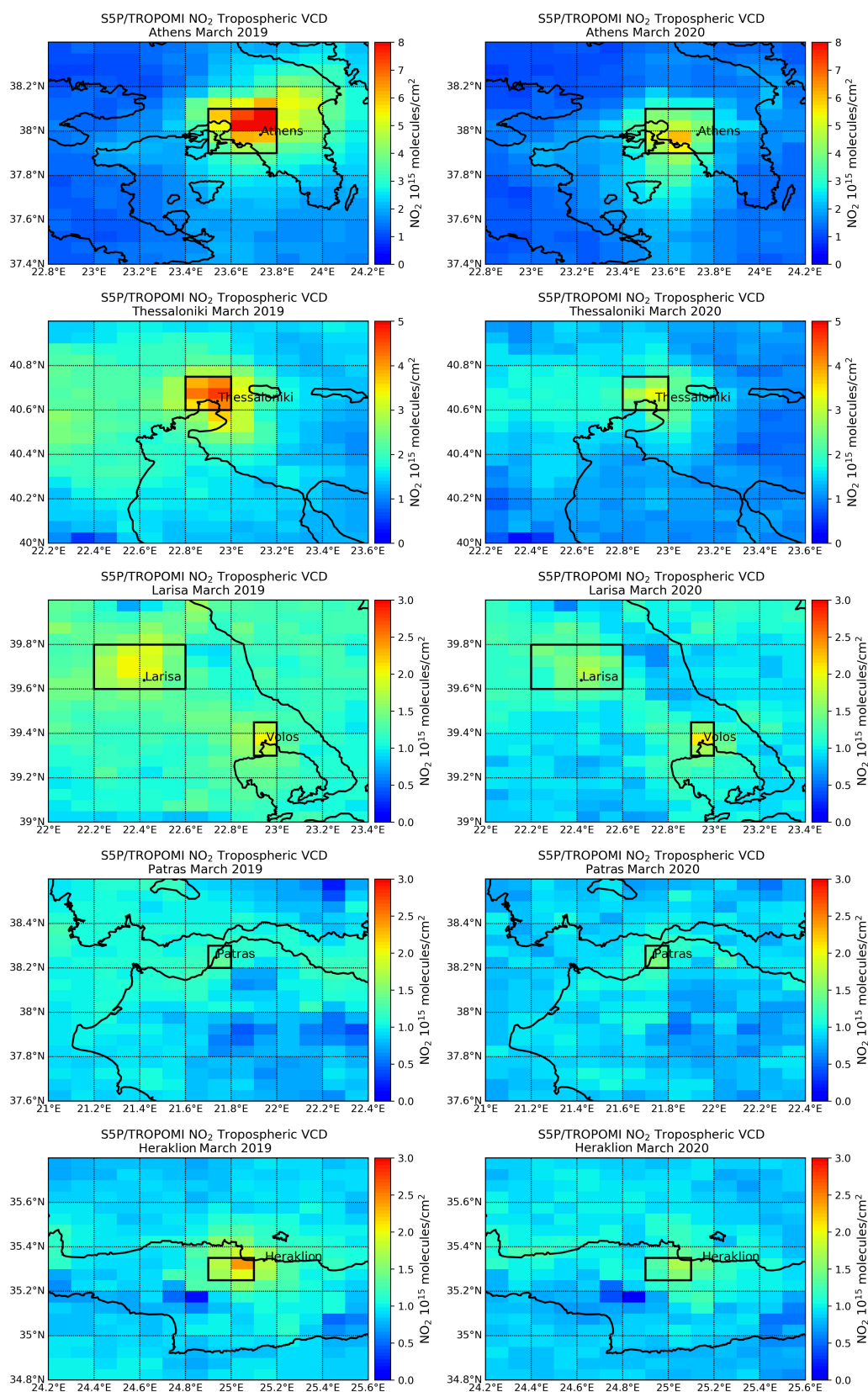


**Figure 2.** Monthly mean TROPOMI tropospheric NO<sub>2</sub> columns (in 10<sup>15</sup> molec. cm<sup>-2</sup>) for March 2019 (left) and March 2020 (right) for the five major cities in Greece. First row, Athens; second row, Thessaloniki; third row, Larisa and Volos; fourth row, Patras; fifth row, Heraklion. The boxes mark the pixels used in the numerical analysis.

In the following sections, we focus on specific hotspot locations and introduce numerical findings.

In Fig. 2, the monthly mean TROPOMI tropospheric NO<sub>2</sub> columns (in 10<sup>15</sup> molec. cm<sup>-2</sup>) are depicted for March 2019 (left) and 2020 (right) for six major cities in Greece: from top to bottom, Athens (37.98° N, 23.72° E), Thessaloniki (40.64° N, 22.94° E), Larisa (39.63° N, 22.41° E), Volos (39.36° N, 22.95° E), Patras (38.24° N, 21.73° E) and Heraklion (35.33° N, 25.14° E). We focus on the locations where major transport emissions are expected, as these six cities, according to the HAS (2011) census, host 4.45 million of the 10.8 million people that make up the Greek population (Table S1 in the Supplement). Even though the NO<sub>2</sub> levels are low over the four smaller cities, we were interested in examining the ability of TROPOMI with respect to sensing both the load and expected changes for these relatively clean cities (numerical results are given in Table 1). The equivalent maps for April 2019 and 2020 are presented in Fig. S1.

In Fig. 3, the monthly mean TROPOMI tropospheric NO<sub>2</sub> columns (in 10<sup>15</sup> molec. cm<sup>-2</sup>) for March (Fig. 3a) and April (Fig. 3b) for 2019 (blue) and 2020 (orange) are shown for the six major cities in Greece: from left to right, Athens, Thessaloniki, Larisa, Volos, Patras and Heraklion. Overall, the NO<sub>2</sub> levels are higher in March for both years (than for the equivalent April months) and are proportional to the cities' populations, with Athens and Thessaloniki showing the highest levels whereas the remaining four cities present similar NO<sub>2</sub> loading conditions. Hence, it is not surprising considering these rather low monthly mean reported satellite estimates, which approach the level of detectability of the satellite sensor, that the changes vary widely from one location to the next and not always in the expected manner. We note here that the associated standard deviation on the monthly mean levels for the four smaller cities is quite large and might affect the robustness of findings later on in this work. In Table 1, the full statistics that relate to Fig. 3 are given, and they show that for the month of March, the relative differences in NO<sub>2</sub> loading sensed by the satellite sensor between 2019 and 2020 range from -3 % to -34 % in all cases except for the port city of Patras, where absolute changes of 0.12 × 10<sup>15</sup> molec. cm<sup>-2</sup> result in percentage differences of +20 %. Similarly, for the month of April, relative changes range from -39 % to +5 %; however, these changes mostly result from extremely small absolute changes of 0.06 × 10<sup>15</sup> molec. cm<sup>-2</sup> (Athens) or 0.08 × 10<sup>15</sup> molec. cm<sup>-2</sup> (Volos). The equivalent bar plot for the CTM tropospheric NO<sub>2</sub> columns is given in Fig. S2, in the same format as Fig. 3, and the relevant statistics are shown in Table S2. We note that, for the possible available observations per location, for the month of March there were slightly fewer available pixels for 2020 than for 2019, on average ~ -15 % with a range between -5 % and -22 %, with the highest difference for Thessaloniki, which was overcast the entire final week of March 2020, as previously discussed.

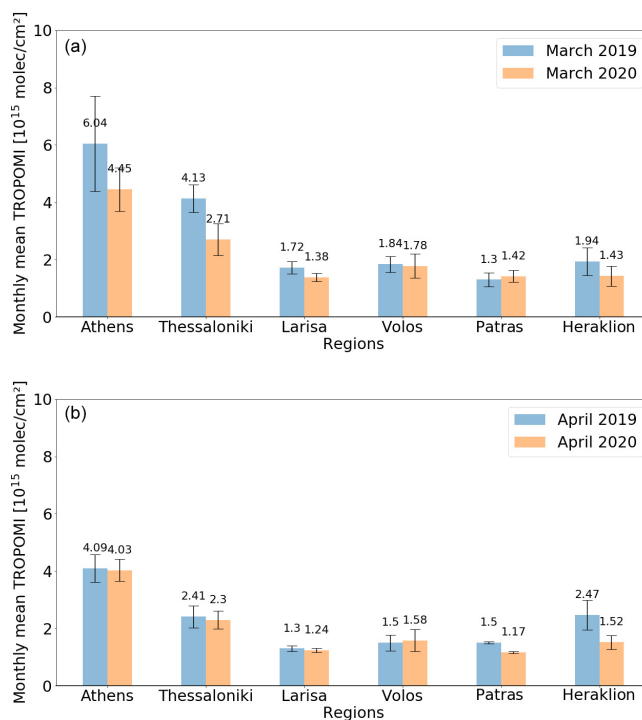


**Figure 3.** Monthly mean TROPOMI tropospheric NO<sub>2</sub> columns (in 10<sup>15</sup> molec. cm<sup>-2</sup>) for March (a) and April (b) for 2019 (blue) and 2020 (orange) for the five major cities in Greece: from left to right, Athens, Thessaloniki, Larisa, Volos, Patras and Heraklion.

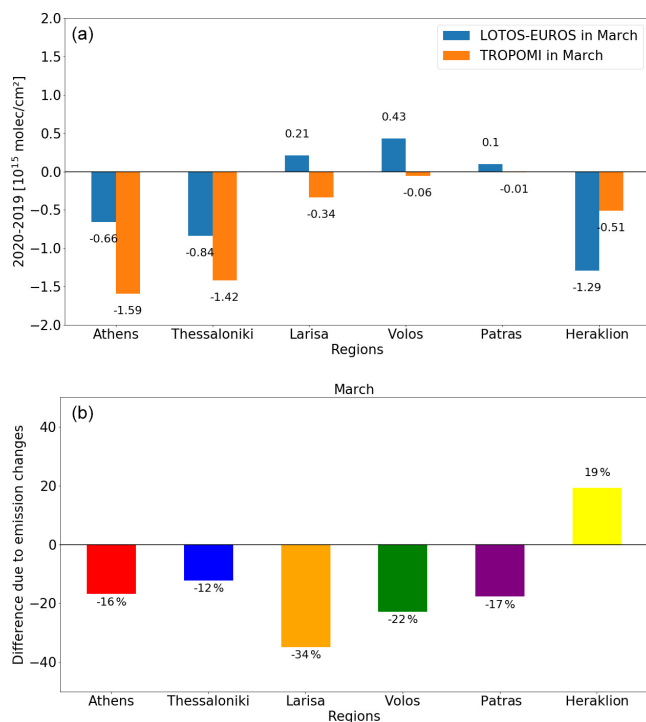
For April, slightly more pixels were available for 2020, on average +5 % with a range between 1 % and 11 %.

In Fig. 4a, the monthly mean absolute differences in tropospheric NO<sub>2</sub> columns (10<sup>15</sup> molec. cm<sup>-2</sup>) between 2020 and 2019 are shown for TROPOMI (orange) and LOTOS-EUROS (blue) for the six major cities in Greece: Athens, Thessaloniki, Larisa, Volos, Patras and Heraklion. We opted to show absolute differences here, and not percentage differences as might be expected, as a small relative change in a low NO<sub>2</sub> abundance would result in the erroneous message of a large reduction, as has already been shown in Fig. 3. In Fig. 4b, the emission changes are quantified in the following manner: the percentage differences for LOTOS-EUROS between 2019 and 2020 are calculated as the equivalent percentage differences seen by TROPOMI. By subtracting one percentage difference from the other (and not directly comparing the two), the actual NO<sub>2</sub> emission reduction may be quantified.

This percentage difference is found to be -16 % for Athens, -12 % for Thessaloniki, -34 % for Larisa, -22 % for Volos, -17 % for Patras and +19 % for Heraklion. This study shows that, for relatively low tropospheric NO<sub>2</sub> columns of the order of 1.5 × 10<sup>15</sup> molec. cm<sup>-2</sup>, this methodology, which is based on differences, may result in unexpected numerical findings. Similar studies that have examined the effects of the COVID-19 lockdown on air qual-

**Table 1.** Monthly mean TROPOMI NO<sub>2</sub> levels (10<sup>15</sup> molec. cm<sup>-2</sup>) over major cities in Greece for March (left block) and April (right block) for 2019 and 2020 as well as their relative difference, standard deviation and number of pixels (in parentheses).

Location	March 2019	March 2020	Percent diff.	April 2019	April 2020	Percent diff.
Athens (12)	6.04 ± 1.65	4.45 ± 0.76	-26 %	4.09 ± 0.49	4.03 ± 0.38	-1 %
Thessaloniki (6)	4.13 ± 0.34	2.71 ± 0.38	-34 %	2.41 ± 0.28	2.30 ± 0.22	-5 %
Larisa (16)	1.72 ± 0.22	1.38 ± 0.17	-19 %	1.30 ± 0.13	1.24 ± 0.09	-5 %
Volos (3)	1.84 ± 0.13	1.78 ± 0.21	-3 %	1.50 ± 0.14	1.58 ± 0.19	+5 %
Patras (2)	1.30 ± 0.10	1.42 ± 0.19	+20 %	1.50 ± 0.02	1.17 ± 0.01	-18 %
Heraklion (4)	1.94 ± 0.29	1.43 ± 0.08	-26 %	2.47 ± 0.30	1.52 ± 0.14	-39 %

**Figure 4.** (a) Monthly mean absolute differences in tropospheric NO<sub>2</sub> columns (in 10<sup>15</sup> molec. cm<sup>-2</sup>) between 2020 and 2019 are shown for TROPOMI (orange) and LOTOS-EUROS (blue) for the five major cities in Greece: from left to right, Athens, Thessaloniki, Larisa, Volos, Patras and Heraklion. (b) The percentage differences that may be attributable to emission changes.

ity based on satellite observations have focused on eastern China, specific US and Canadian locations and the Po Valley in Italy, which observe orders of magnitude higher tropospheric NO<sub>2</sub> columns even during the reduced emissions period. As a result, our main tentative finding is that a  $\sim -10\%$  reduction in tropospheric NO<sub>2</sub> columns as sensed by the S5P/TROPOMI instrument over Greece may be attributed to the reduced emissions due to the COVID-19 pandemic. Hence, we continue this study focusing only on the location with the highest observed tropospheric NO<sub>2</sub> columns – the

capital city of Athens – at a weekly temporal scale, so as to refine this estimate.

### 3.2 Lockdown effects on weekly NO<sub>2</sub> levels over Athens

Without disregarding the possible contribution of central heating to total NO<sub>x</sub> emissions, the largest decrease due to the COVID-19 lockdown is indeed observed over the main Greek hotspot, the city of Athens and its surroundings. In Fig. 5, weekly mean TROPOMI tropospheric NO<sub>2</sub> columns (in 10<sup>15</sup> molec. cm<sup>-2</sup>) over Athens for 2019 (left) and 2020 (right) are shown for 15–21 March (first row), 8–14 April (second row), 15–21 April (third row) and 22–28 April (fourth row). Apart from the obvious reduction in magnitude during the lockdown months, the effect of the winds for both the location of the local maximum and the spread of the pollution plume is most prominent in this composite, which further strengthens our decision not to perform one-to-one comparisons between the different NO<sub>2</sub> fields. The average weekly NO<sub>2</sub> load over Athens sensed by TROPOMI is presented in a numerical form in Fig. 6, where the 2019 averages are shown in blue and the 2020 averages are shown in orange for the weeks of March and April. Out of the 12 pixels considered for this subdomain, which may provide up to 84 measurements for each week in the case of clear skies, for the year 2019 an average of  $53 \pm 16$  (median of 52) clear-sky S5P/TROPOMI observations were found, whereas for the year 2020, an average of  $52 \pm 25$  (median of 56) clear-sky S5P/TROPOMI observations were found. Even though the representativeness of the weekly levels can by no means be considered equal between the years, apart from the penultimate week, TROPOMI reports lower NO<sub>2</sub> columns ranging between  $-8\%$  and  $-43\%$ . The MAXDOAS observations over Athens also show a very similar behaviour, reporting  $6.77 \pm 6.85 \times 10^{15}$  and  $3.60 \pm 1.83 \times 10^{15}$  molec. cm<sup>-2</sup> for March and April 2019 respectively and  $2.76 \pm 3.17$  and  $2.77 \pm 2.44 \times 10^{15}$  molec. cm<sup>-2</sup> for March and April 2020 respectively, showing a much larger reduction for the month of March than for the month of April.

The meteorology over these 8 weeks over Athens shows that, temperature-wise, the entire month of March 2019 as well as the first 3 weeks of April had very similar levels with a very hot spell affecting the last week of April 2019,

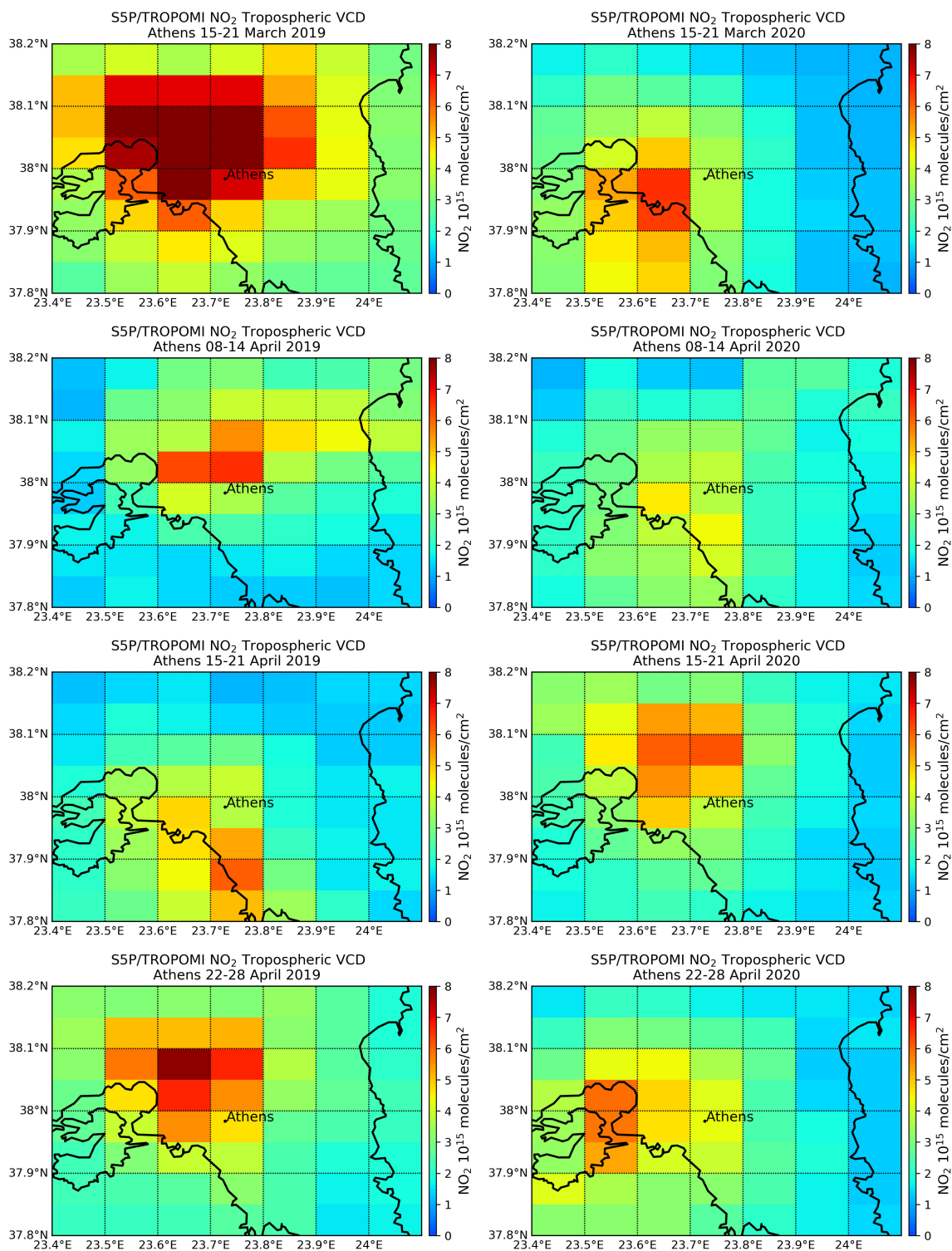


**Figure 5.** Weekly mean TROPOMI tropospheric NO<sub>2</sub> columns (in 10<sup>15</sup> molec. cm<sup>-2</sup>) over Athens for 2019 (left) and 2020 (right): first row, 15–21 March 2019; second row, 8–14 April; third row, 15–21 April; fourth row, 22–28 April.

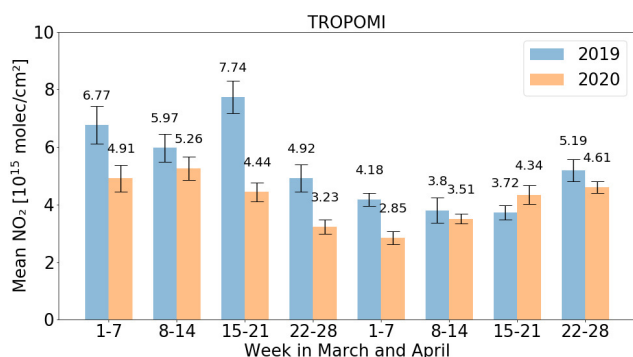


**Figure 6.** Weekly mean TROPOMI tropospheric NO<sub>2</sub> columns (in 10<sup>15</sup> molec. cm<sup>-2</sup>) for weeks in 2019 (blue) and 2020 (orange) for Athens.

which was also Easter Week in Greece. In 2020, a cold front appeared during the third week of March which lasted until mid-April when warmer weather appeared and remained (Fig. S5). The mean vector wind speed and direction, overlain as arrows in Fig. S5, are very similar with mostly predominant northern winds and very few cases of southerly winds. In the equivalent rose diagrams (Fig. S6), we again note that the main wind directions appear similar between the two periods (2019 in the left column and 2020 in the right column) apart from the last week of April (bottom row) where the two weeks had very different directions for the same magnitude. Note that the percentiles are not constant between rose diagrams.

A question that often arises when examining a relatively short time period of a highly varying atmospheric species is whether the period considered as “normal” was indeed normal from a climatological point of view. We have opted to create a climatological mean based on the daily OMI/Aura NO<sub>2</sub> cloud-screened tropospheric column L3 global gridded 0.25 × 0.25° v003 product (Krotkov et al., 2017, 2019), accessed from the NASA EarthData Giovanni repository. The monthly variability of the tropospheric NO<sub>2</sub> load over Athens for 2019 (blue) and 2020 (orange) is shown in Fig. 7a as the percentage difference from the climatological mean (grey shaded area). As is also observed by the TROPOMI instrument, the OMI observations reveal a higher decrease for March 2020 compared with March 2019 (than the equivalent decrease for the April months). In Fig. 7b, the weekly variability of the tropospheric NO<sub>2</sub> load over Athens for 2019 (blue) and 2020 (orange) is shown, starting in the first week of March and covering 8 weeks. It is also shown in this representation that the weeks of March in 2020 were further from the climatological mean compared with the weeks in April 2020, whereas the April 2019 weeks present overall lower NO<sub>2</sub> loads, as also shown by TROPOMI (Fig. 6).

Another question that is also often discussed when examining such abrupt changes in localized emission sources is whether in situ surface measurements depict the changes in

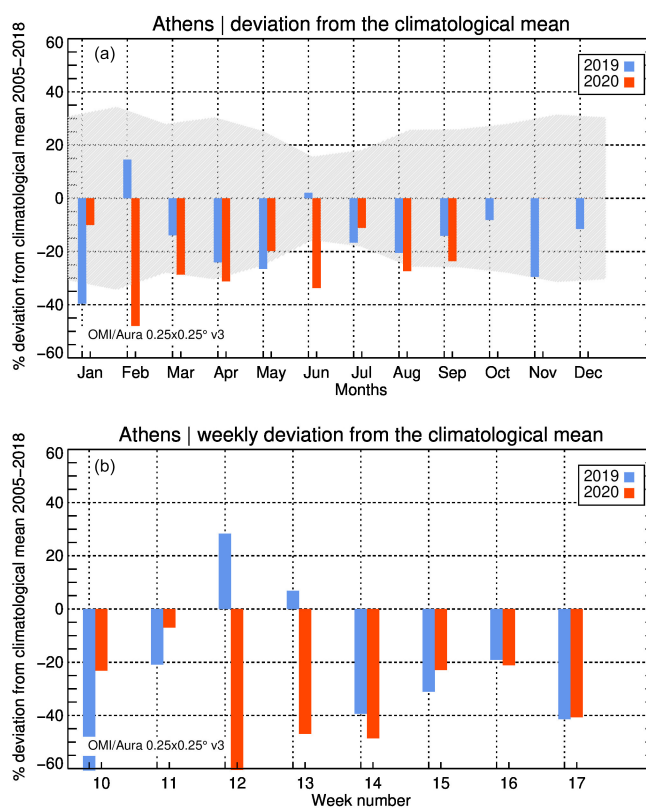


**Figure 7.** (a) The OMI/Aura v003 L3 gridded cloud-screened tropospheric NO<sub>2</sub> monthly deviations from the climatological mean (grey shaded area) for 2019 (in blue) and 2020 (in orange). (b) The OMI/Aura v003 L3 gridded cloud-screened tropospheric NO<sub>2</sub> weekly deviations from the climatological mean for 2019 (in blue) and 2020 (in orange) starting in week 10, the first week of March.

the same order and magnitude. For the case of the COVID-19 pandemic, a number of studies of European locations have appeared with surprising findings; in Ropkins and Tate (2021), measurements from automated monitoring stations across the UK showed abrupt NO<sub>2</sub> decreases at the onset of the UK lockdown, between ~ 25 % and 50 % at urban traffic and urban background stations. Surprisingly, after the initial abrupt reduction, gradual increases were then observed throughout the rest of the UK lockdown period. A similar finding is reported by Dacre et al. (2020), who showed that the in situ air quality stations in the north and middle of England measured a decrease in NO<sub>2</sub> concentrations in the lockdown period from 17 March to 30 April 20, whereas stations in the south of England measured an increase in NO<sub>2</sub> concentrations. Putaud et al. (2020) studied in situ concentrations from an urban background and a regional background station in the north of Italy and showed that the NO<sub>2</sub> concentrations decreased as a consequence of the lockdown by –30 % and –40 % on average respectively.

For the purposes of this discussion, we have analysed the in situ surface  $\text{NO}_2$  measurements reported by seven air quality stations around Athens (locations shown in Fig. S3), and their individual monthly mean variability for 12:00 UTC is shown in Fig. S4. These long-term observations are maintained by the Greek Ministry Environment and Energy (YPEKA) network who further report them to the EEA, and they are officially designated as industrial, urban and suburban locations. The measurement time closest to the TROPOMI overpass time over Athens was chosen to calculate a climatology between 2005 and 2018, and the monthly mean  $\text{NO}_2$  levels calculated from the time series shown in Fig. S4 are presented in Fig. 8a. The grey line and shaded area show the seasonal variability of the mean surface concentrations (in  $\mu\text{g m}^{-3}$ ) with higher levels during wintertime months and lower levels during summertime. Similar  $\text{NO}_2$  concentrations are reported for the month of March in 2019 (in blue) and 2020 (in purple), at the lower statistical level, whereas an unexpected increase for April (and May) 2019 shows a large difference to the lows found in April 2020, which was the full COVID lockdown month for Greece. This finding is clearer in Fig. 8b, where the monthly deviation of 2019 (in blue) and 2020 (in orange) are given as bars overlaid against the grey shaded area that shows the variability of the climatological means. Thus, contrary to what the space-borne observations by both TROPOMI and OMI as well as the ground-based MAXDOAS measurements show, the in situ measurements report a similar difference to the climatological mean for the months of March, whereas April 2019 appears in the positive range and April 2020 is beyond the lower statistical level. Grivas et al. (2020) compared climatological hourly  $\text{NO}_2$  concentrations measured by an urban background station in the Athens Basin (not included in our work) for the years 2016–2020 to days corresponding to the pre-lockdown (1–22 March), lockdown (23 March–10 May) and post lockdown (11–31 May) periods of 2020. Overall, they report  $-6\%$ ,  $-41.5\%$  and  $+8.7\%$  changes between 2020 and the 2016–2020 equivalent periods.

The contribution of the meteorological factors to the observed tropospheric  $\text{NO}_2$  load can be assessed by the equivalent LOTOS-EUROS weekly averages, shown Fig. 9a. As in Fig. 4b, the percentage differences of the LOTOS-EUROS simulations between 2019 and 2020 are calculated, as were those for the TROPOMI equivalent weekly means (Fig. 6). The difference between those two relative differences is given in Fig. 9b. The fact that the CTM predicted an increase in  $\text{NO}_2$  production for most weeks, under the assumption that the primary emissions remained stable between the 2 years, results in higher reduction levels ranging between  $-24\%$  and  $-66\%$  for 5 of the 8 weeks studied, whereas an assumed increase in emissions is calculated for the remaining 3 weeks with levels between  $+4\%$  and  $+10\%$ . These increases in emission levels, which are not corroborated by the in situ observations, give us an estimate on the uncertainty of this methodology ( $\sim 10\%$ ). Even so, the average difference

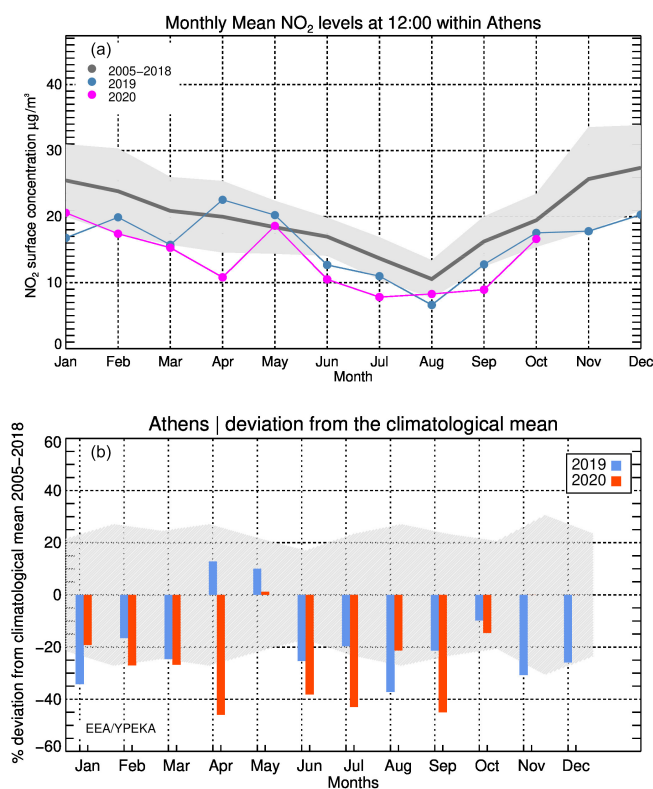


**Figure 8.** (a) Monthly mean  $\text{NO}_2$  surface concentrations (in  $\mu\text{g m}^{-3}$ ) for the climatological mean of 2005 to 2018 (dark grey line) with the standard deviation (grey shaded area), 2019 (in blue) and 2020 (in purple) calculated from the levels reported by seven air quality stations, as shown in Fig. S4. (b) The monthly percentage deviation from the climatological mean (shaded grey area) for the months of 2019 (blue) and 2020 (orange).

in emissions over Athens for these 8 weeks is calculated at  $\sim -20\%$  from the S5P/TROPOMI tropospheric  $\text{NO}_2$  observations.

## 4 Conclusions

In this work, Sentinel-5P/TROPOMI tropospheric  $\text{NO}_2$  observations were studied in order to examine the possible positive effect on Greek air quality caused by the recent COVID-19 pandemic lockdown. The country enforced severe movement restrictions, and entire economic sectors were gradually shut down, starting from the last weekend of February, before total lockdown came into effect beginning on Monday 23 March and ending on 4 May. The time period between March and April 2020 and the equivalent weeks in 2019 were analysed and compared on a monthly basis for six of the most populous cities in Greece. TROPOMI monthly mean tropospheric nitrogen dioxide ( $\text{NO}_2$ ) observations showed a change of between  $-34\%$  and  $+20\%$  and between  $-39\%$  and  $+5\%$  with an average of  $-15\%$  and

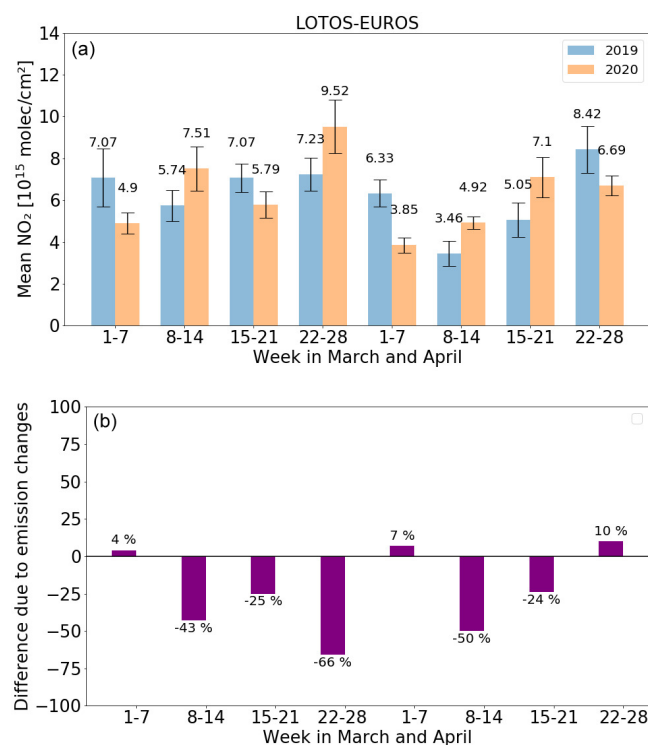


**Figure 9.** (a) Weekly mean LOTOS-EUROS tropospheric NO<sub>2</sub> columns (in 10<sup>15</sup> molec. cm<sup>-2</sup>) for weeks in 2019 (blue) and 2020 (orange) for Athens. (b) The percentage differences attributed to emission changes, revealing the actual magnitude of the NO<sub>x</sub> emissions decrease.

–11 % for March and April 2020 respectively, compared with the previous year, for the urban areas, which was mostly attributable to vehicular emission reductions. For the capital city of Athens, weekly reductions in the TROPOMI tropospheric NO<sub>2</sub> columns (between –8 % and –43 %) for 7 of the 8 weeks studied were found, corroborated by the spaceborne OMI/Aura observations and ground-based multi-axis differential optical absorption spectroscopy (MAXDOAS) measurements. Stronger reductions were reported by seven in situ air quality stations in Athens that reported measurements to the European Environment Agency Air Quality database, with monthly decreases reaching –40 % for the month of April 2020. In order to eliminate the expected meteorological effects on the observed NO<sub>2</sub> levels, chemical transport modelling simulations, provided by the LOTOS-EUROS CTM, show that the magnitude of these satellite-sensed reductions cannot solely be attributed to the difference in meteorological factors affecting NO<sub>2</sub> levels during March and April 2020 and the equivalent time periods of the previous year. Taking this factor into account, the resulting decline due to the COVID-19 related measures was estimated to range between –10 % and –20 % for the different spatio-temporal scales studied in this work, taking into account the possible uncertainties of the methodology con-

sidering the low tropospheric NO<sub>2</sub> levels observed around Greece.

**Data availability.** The S5P data used here are publicly available from the Copernicus Open Access Hub (<https://scihub.copernicus.eu/>, ESA, 2021). The LOTOS-EUROS simulations are available upon request. The air quality monitoring station data are publicly available via the European Environment Agency Air Quality monitoring service, <https://discomap.eea.europa.eu/map/fine/AirQualityExport.htm> (EEA, 2021) and the Greek Ministry of the Environment and Energy monitoring network, <https://ypen.gov.gr/perivallon/poiotita-tis-atmosfairas/dedomena-metriseon-atmosfairikis-rypansis/> (Greek Ministry of the Environment, 2021). The OMI/Aura NO<sub>2</sub> cloud-screened tropospheric column L3 global gridded 0.25 × 0.25° v003 product is publicly available from the NASA EarthData Giovanni repository, <https://giovanni.gsfc.nasa.gov/giovanni/> (NASA, 2021). The MAXDOAS observations discussed in this text are publicly available from <https://mpc-vdaf-server.tropomi.eu/no2/no2-offl-maxdoas/athens> (MPC ESA, 2021).

**Supplement.** The supplement related to this article is available online at: <https://doi.org/10.5194/acp-21-1759-2021-supplement>.

**Author contributions.** The data analysis was performed by IS, AK and MEK. Methodology and conceptualization was undertaken by DB and IP. Software development was carried out by IS and AK. MEK wrote and prepared the original draft of the paper, and DB, AS, AM, JvG and HE reviewed and edited it. All authors read and agreed on the published version of the paper.

**Competing interests.** The authors declare that they have no conflict of interest.

**Acknowledgements.** We acknowledge the usage of modified Copernicus Sentinel data (2019–2020). Results presented in this work have been produced using the Aristotle University of Thessaloniki (AUTH) high-performance computing infrastructure and resources. Maria-Elissavet Koukouli, Ioanna Skoulidou and Dimitris Balis would like to acknowledge the support provided by the IT Center of the AUTH throughout the progress of this research work. Maria-Elissavet Koukouli and Andreas Karavias would also like to acknowledge the support provided by the Atmospheric Toolbox<sup>®</sup>.

**Financial support.** This research has been supported by the European Union (European Regional Development Fund), Greek national funds through the “Competitiveness, Entrepreneurship and Innovation” operational programme (grant no. NSRF 2014-2020), the “Panhellenic Infrastructure for Atmospheric Composition and Climate Change” project (grant no. MIS 5021516) and the “Innovative system for Air Quality Monitoring and Forecasting” project (code T1EDK-01697, grant no. MIS 5031298), implemented under

the Action “Reinforcement of the Research and Innovation” infrastructure.

*Review statement.* This paper was edited by Stelios Kazadzis and reviewed by two anonymous referees.

## References

- Bauwens, M., Compernelle, S., Stavrakou, T., Müller, J.-F., van Gent, J., Eskes, H., Levelt, P. F., van der A, R., Veeffkind, J. P., Vlietinck, J., Yu, H., and Zehner, C.: Impact of coronavirus outbreak on NO<sub>2</sub> pollution assessed using TROPOMI and OMI observations, *Geophys. Res. Lett.*, 47, e2020GL087978, <https://doi.org/10.1029/2020GL087978>, 2020.
- Beirle, S., Boersma, K. F., Platt, U., Lawrence, M. G., and Wagner, T.: Megacity emissions and lifetimes of nitrogen oxides probed from space, *Science*, 333, 1737–1739, <https://doi.org/10.1126/science.1207824>, 2011.
- Blechschmidt, A.-M., Arteta, J., Coman, A., Curier, L., Eskes, H., Foret, G., Gielen, C., Hendrick, F., Marécal, V., Meleux, F., Parmentier, J., Peters, E., Pinardi, G., Piter, A. J. M., Plu, M., Richter, A., Segers, A., Sofiev, M., Valdebenito, Á. M., Van Roozendael, M., Vira, J., Vlemmix, T., and Burrows, J. P.: Comparison of tropospheric NO<sub>2</sub> columns from MAX-DOAS retrievals and regional air quality model simulations, *Atmos. Chem. Phys.*, 20, 2795–2823, <https://doi.org/10.5194/acp-20-2795-2020>, 2020.
- Boersma, K. F., Eskes, H. J., Dirksen, R. J., van der A, R. J., Veeffkind, J. P., Stammes, P., Huijnen, V., Kleipool, Q. L., Sneep, M., Claas, J., Leitão, J., Richter, A., Zhou, Y., and Brunner, D.: An improved tropospheric NO<sub>2</sub> column retrieval algorithm for the Ozone Monitoring Instrument, *Atmos. Meas. Tech.*, 4, 1905–1928, <https://doi.org/10.5194/amt-4-1905-2011>, 2011.
- Boersma, K. F., Eskes, H. J., Richter, A., De Smedt, I., Lorente, A., Beirle, S., van Geffen, J. H. G. M., Zara, M., Peters, E., Van Roozendael, M., Wagner, T., Maasakkers, J. D., van der A, R. J., Nightingale, J., De Rudder, A., Irie, H., Pinardi, G., Lambert, J.-C., and Compernelle, S. C.: Improving algorithms and uncertainty estimates for satellite NO<sub>2</sub> retrievals: results from the quality assurance for the essential climate variables (QA4ECV) project, *Atmos. Meas. Tech.*, 11, 6651–6678, <https://doi.org/10.5194/amt-11-6651-2018>, 2018.
- Castellanos, P. and Boersma, K.: Reductions in nitrogen oxides over Europe driven by environmental policy and economic recession, *Sci. Rep.*, 2, 265, <https://doi.org/10.1038/srep00265>, 2012.
- Cersosimo, A., Serio, C., and Masiello, G.: TROPOMI NO<sub>2</sub> Tropospheric Column Data: Regridding to 1 km Grid-Resolution and Assessment of their Consistency with In Situ Surface Observations, *Remote Sens.*, 12, 2212, <https://doi.org/10.3390/rs12142212>, 2020.
- Curier, R. L., Timmermans, R., Calabretta-Jongen, S., Eskes, H., Segers, A., Swart, D., and Schaap, M.: Improving ozone forecasts over Europe by synergistic use of the LOTOS-EUROS chemical transport model and in-situ measurements, *Atmos. Environ.*, 60, 217–226, <https://doi.org/10.1016/j.atmosenv.2012.06.017>, 2012.
- Curier, R. L., Kranenburg, R., Segers, A. J. S., Timmermans, R. M. A., and Schaap, M.: Synergistic use of OMI NO<sub>2</sub> tropospheric columns and LOTOS-EUROS to evaluate the NO<sub>x</sub> emission trends across Europe, *Remote Sens. Environ.*, 149, 58–69, <https://doi.org/10.1016/j.rse.2014.03.032>, 2014.
- Dacre, H. F., Mortimer, A. H., and Neal, L. S.: How have surface NO<sub>2</sub> concentrations changed as a result of the UK’s COVID-19 travel restrictions? *Environ. Res. Lett.*, 15, 104089, <https://doi.org/10.1088/1748-9326/abb6a2>, 2020.
- Ding, J., van der A, R. J., Mijling, B., Levelt, P. F., and Hao, N.: NO<sub>x</sub> emission estimates during the 2014 Youth Olympic Games in Nanjing, *Atmos. Chem. Phys.*, 15, 9399–9412, <https://doi.org/10.5194/acp-15-9399-2015>, 2015.
- Ding, J., van der A, R. J., Eskes, H. J., Mijling, B., Stavrakou, T., van Geffen, J. H. G. M., and Veeffkind, P. J.: NO<sub>x</sub> emissions reduction and rebound in China due to the COVID-19 crisis, *Geophys. Res. Lett.*, 46, e2020GL089912, <https://doi.org/10.1029/2020GL089912>, 2020.
- Eskes, H. J. and Boersma, K. F.: Averaging kernels for DOAS total-column satellite retrievals, *Atmos. Chem. Phys.*, 3, 1285–1291, <https://doi.org/10.5194/acp-3-1285-2003>, 2003.
- European Environment Agency (EEA): Air quality in Europe – 2019 report, <https://doi.org/10.2800/822355>, 2019a.
- European Environment Agency (EEA): Report No 8/2019, European Union emission inventory report 1990–2017 under the UNECE Convention on Long-range Transboundary Air Pollution (LRTAP), <https://doi.org/10.2800/78220>, 2019b.
- European Environment Agency (EEA): Air quality measurements from in situ monitoring stations, available at: <https://discomap.eea.europa.eu/map/fme/AirQualityExport.htm>, last access: 3 February 2021.
- European Space Agency (ESA): Sentinel-5P Pre-Operations Data Hub, available at: <https://scihub.copernicus.eu/>, last access: 3 February 2021.
- European Union (EU): The Environmental Implementation Review 2019, COUNTRY REPORT: GREECE, available at: [https://ec.europa.eu/environment/eir/pdf/report\\_el\\_en.pdf](https://ec.europa.eu/environment/eir/pdf/report_el_en.pdf) (last access: 30 April 2020), 2019.
- Fameli, K. M. and Assimakopoulos, V. D.: Development of a road transport emission inventory for Greece and the Greater Athens Area: Effects of important parameters, *Sci. Total Environ.*, 505, 770–786, <https://doi.org/10.1016/j.scitotenv.2014.10.015>, 2015.
- Fountoukis, C. and Nenes, A.: ISORROPIA II: a computationally efficient thermodynamic equilibrium model for K<sup>+</sup>–Ca<sup>2+</sup>–Mg<sup>2+</sup>–NH<sub>4</sub><sup>+</sup>–Na<sup>+</sup>–SO<sub>4</sub><sup>2-</sup>–NO<sub>3</sub><sup>-</sup>–Cl<sup>-</sup>–H<sub>2</sub>O aerosols, *Atmos. Chem. Phys.*, 7, 4639–4659, <https://doi.org/10.5194/acp-7-4639-2007>, 2007.
- Gery, M. W., Whitten, G. Z., Killus, J. P., and Dodge, M. C.: A photochemical kinetics mechanism for urban and regional scale computer modeling, *J. Geophys. Res.*, 94, 12925–12956, <https://doi.org/10.1029/JD094iD10p12925>, 1989.
- Goldberg, D. L., Anenberg, S. C., Griffin, D., McLinden, C. A., Lu, Z., and Streets, D. G.: Disentangling the impact of the COVID-19 lockdowns on urban NO<sub>2</sub> from natural variability, *Geophys. Res. Lett.*, 47, e2020GL089269, <https://doi.org/10.1029/2020GL089269>, 2020.
- Greek Ministry of the Environment: Air quality measurements from in situ monitoring stations, available at: <https://ypen.gov.gr/perivallon/poiotita-tis-atmosfairas/>

- dedomena-metriseon-atmosfairikis-rypanis/, last access: 3 February 2021.
- Grivas, G., Athanasopoulou, E., Kakouri, A., Bailey, J., Liakakou, E., Stavroulas, I., Kalkavouras, P., Bougiatioti, A., Kaskaoutis, D.G., Ramonet, M., Mihalopoulos, N., and Gerasopoulos, E.: Integrating in situ Measurements and City Scale Modelling to Assess the COVID-19 Lockdown Effects on Emissions and Air Quality in Athens, Greece, *Atmosphere*, 11, 1174, <https://doi.org/10.3390/atmos11111174>, 2020.
- Hellenic Statistical Authority (HAS): 2011 Population-Housing Census, available at: <https://www.statistics.gr/2011-census-pop-hous> (last access: 7 December 2020), 2011.
- Hellenic Statistical Authority (HAS): Air Emission Accounts, available at: <https://www.statistics.gr/en/statistics/-/publication/SOP08/> (last access: 7 February 2020), 2017.
- Ialongo, I., Virta, H., Eskes, H., Hovila, J., and Douros, J.: Comparison of TROPOMI/Sentinel-5 Precursor NO<sub>2</sub> observations with ground-based measurements in Helsinki, *Atmos. Meas. Tech.*, 13, 205–218, <https://doi.org/10.5194/amt-13-205-2020>, 2020.
- Independent Power Transmission Operator (IPTO): Monthly Energy Reports, available at: <https://www.admie.gr/en/market/reports/monthly-energy-balance>, last access: 7 February 2020.
- Jacob, D. J.: Introduction to Atmospheric Chemistry, Princeton University Press, ISBN 10 0691001855, available at: <https://press.princeton.edu/books/hardcover/9780691001852/introduction-to-atmospheric-chemistry> (last access: 8 February 2021), 1999.
- Jacob, D. J. and Winner, D. A.: Effect of climate change on air quality, *Atmos. Environ.*, 43, 51–63, <https://doi.org/10.1016/j.atmosenv.2008.09.051>, 2009.
- Krotkov, N. A., Lamsal, L. N., Celarier, E. A., Swartz, W. H., Marchenko, S. V., Bucsela, E. J., Chan, K. L., Wenig, M., and Zara, M.: The version 3 OMI NO<sub>2</sub> standard product, *Atmos. Meas. Tech.*, 10, 3133–3149, <https://doi.org/10.5194/amt-10-3133-2017>, 2017.
- Krotkov, N. A., Lok, N., Lamsal, S., Marchenko, V., Celarier, E. A., Bucsela, E. J., Swartz, W. H., Joiner, J., and the OMI core team: OMI/Aura NO<sub>2</sub> Cloud-Screened Total and Tropospheric Column L3 Global Gridded 0.25 degree x 0.25 degree V3, NASA Goddard Space Flight Center, Goddard Earth Sciences Data and Information Services Center (GES DISC), <https://doi.org/10.5067/Aura/OMI/DATA3007>, 2019.
- Kuenen, J. J. P., Visschedijk, A. J. H., Jozwicka, M., and Denier van der Gon, H. A. C.: TNO-MACC-II emission inventory; a multi-year (2003–2009) consistent high-resolution European emission inventory for air quality modelling, *Atmos. Chem. Phys.*, 14, 10963–10976, <https://doi.org/10.5194/acp-14-10963-2014>, 2014.
- Lamsal, L. N., Martin, R. V., van Donkelaar, A., Celarier, E. A., Bucsela, E. J., Boersma, K. F., Dirksen, R., Luo, C., and Wang, Y.: Indirect validation of tropospheric nitrogen dioxide retrieved from the OMI satellite instrument: Insight into the seasonal variation of nitrogen oxides at northern midlatitudes, *J. Geophys. Res.*, 115, D05302, <https://doi.org/10.1029/2009JD013351>, 2010.
- Liu, F., Page, A., Strode, S. A., Yoshida, Y., Choi, S., Zheng, B., Lamsal, L. N., Li, C., Krotkov, N. A., Eskes, H., van der A, R., Veefkind, P., Levelt, P., Joiner, J., and Hauser, O. P.: Abrupt declines in tropospheric nitrogen dioxide over China after the outbreak of COVID-19, *Sci. Adv.*, 6, 28, <https://doi.org/10.1126/sciadv.abc2992>, 2020.
- Lorente, A., Boersma, K. F., Eskes, H. J., Veefkind, J. P., van Geffen, J. H. G. M., de Zeeuw, M. B., Denier van der Gon, H. A. C., Beirle, S., and Krol, M. C.: Quantification of nitrogen oxides emissions from build-up of pollution over Paris with TROPOMI, *Sci. Rep.*, 9, 20033, <https://doi.org/10.1038/s41598-019-56428-5>, 2019.
- Manders, A. M. M., Builtjes, P. J. H., Curier, L., Denier van der Gon, H. A. C., Hendriks, C., Jonkers, S., Kranenburg, R., Kuenen, J. J. P., Segers, A. J., Timmermans, R. M. A., Visschedijk, A. J. H., Wichink Kruit, R. J., van Pul, W. A. J., Sauter, F. J., van der Swaluw, E., Swart, D. P. J., Douros, J., Eskes, H., van Meijgaard, E., van Ulft, B., van Velthoven, P., Banzhaf, S., Mues, A. C., Stern, R., Fu, G., Lu, S., Heemink, A., van Velzen, N., and Schaap, M.: Curriculum vitae of the LOTOS-EUROS (v2.0) chemistry transport model, *Geosci. Model Dev.*, 10, 4145–4173, <https://doi.org/10.5194/gmd-10-4145-2017>, 2017.
- Marécal, V., Peuch, V.-H., Andersson, C., Andersson, S., Arteta, J., Beekmann, M., Benedictow, A., Bergström, R., Bessagnet, B., Cansado, A., Chéroux, F., Colette, A., Coman, A., Curier, R. L., Denier van der Gon, H. A. C., Drouin, A., Elbern, H., Emili, E., Engelen, R. J., Eskes, H. J., Foret, G., Friese, E., Gauss, M., Giannaros, C., Guth, J., Joly, M., Jaumouillé, E., Josse, B., Kadygrov, N., Kaiser, J. W., Krajsek, K., Kuenen, J., Kumar, U., Liora, N., Lopez, E., Malherbe, L., Martinez, I., Melas, D., Meleux, F., Menut, L., Moinat, P., Morales, T., Parmentier, J., Piacentini, A., Plu, M., Poupkou, A., Queguiner, S., Robertson, L., Rouil, L., Schaap, M., Segers, A., Sofiev, M., Tarasson, L., Thomas, M., Timmermans, R., Valdebenito, Á., van Velthoven, P., van Versendaal, R., Vira, J., and Ung, A.: A regional air quality forecasting system over Europe: the MACC-II daily ensemble production, *Geosci. Model Dev.*, 8, 2777–2813, <https://doi.org/10.5194/gmd-8-2777-2015>, 2015.
- Mijling, B. and van der A, R. J.: Using daily satellite observations to estimate emissions of short-lived air pollutants on a mesoscopic scale, *J. Geophys. Res.*, 117, D17302, <https://doi.org/10.1029/2012JD017817>, 2012.
- Mijling, B., van der A, R., Boersma, K. F., Van Roozendaal, M., De Smedt, I., and Kelder, H.: Reductions of NO<sub>2</sub> detected from space during the 2008 Beijing Olympic Games, *Geophys. Res. Lett.* 36, L13801, <https://doi.org/10.1029/2009GL038943>, 2009.
- Miyazaki, K., Bowman, K., Sekiya, T., Jiang, Z., Chen, X., Eskes, H., Ru, M., Zhang, Y., and Shindell, D.: Air quality response in China linked to the 2019 novel coronavirus (COVID-19) lockdown, *Geophys. Res. Lett.*, 47, e2020GL089252, <https://doi.org/10.1029/2020GL089252>, 2020.
- MPC ESA: Sentinel-5P MPC Validation Server, NO<sub>2</sub> tropospheric column OFFL vs MAXDOAS, available at: <https://mpc-vdaf-server.tropomi.eu/no2/no2-offl-maxdoas/athens>, last access: 3 February 2021.
- NASA: EarthData Giovanni repository, available at: <https://giovanni.gsfc.nasa.gov/giovanni/>, last access: 3 February 2021.
- Putaud, J.-P., Pozzoli, L., Pisoni, E., Martins Dos Santos, S., Lagler, F., Lanzani, G., Dal Santo, U., and Colette, A.: Impacts of the COVID-19 lockdown on air pollution at regional and urban background sites in northern Italy, *Atmos. Chem. Phys. Dis-*

- cuss. [preprint], <https://doi.org/10.5194/acp-2020-755>, in review, 2020.
- ROCVR: Quarterly Validation Report of the Sentinel-5 Precursor Operational Data Products #08: April 2018–August 2020, S5P Mission Performance Centre Reference, S5P-MPC-IASB-ROCVR-08.01.01-20200921, #08, 08.01.01, available at: [https://s5p-mpc-vdaf.aeronomie.be/ProjectDir/reports/pdf/S5P-MPC-IASB-ROCVR-08.01.01-20200921\\_FINAL.pdf](https://s5p-mpc-vdaf.aeronomie.be/ProjectDir/reports/pdf/S5P-MPC-IASB-ROCVR-08.01.01-20200921_FINAL.pdf), last access: 17 December 2020.
- Ropkins, K. and Tate, J. E.: Early observations on the impact of the COVID-19 lockdown on air quality trends across the UK, *Sci. Total Environ.*, 745, 142374, <https://doi.org/10.1016/j.scitotenv.2020.142374>, 2021.
- Schaap, M., Kranenburg, R., Curier, L., Jozwicka, M., Dammers, E., and Timmermans, R.: Assessing the Sensitivity of the OMI-NO<sub>2</sub> Product to Emission Changes across Europe, *Remote Sens.*, 5, 4187–4208, <https://doi.org/10.3390/rs5094187>, 2013.
- Seo, J., Kim, J. Y., Youn, D., Lee, J. Y., Kim, H., Lim, Y. B., Kim, Y., and Jin, H. C.: On the multiday haze in the Asian continental outflow: the important role of synoptic conditions combined with regional and local sources, *Atmos. Chem. Phys.*, 17, 9311–9332, <https://doi.org/10.5194/acp-17-9311-2017>, 2017.
- Skoulidou, I., Koukouli, M.-E., Manders, A., Segers, A., Karagiorgidis, D., Gratsea, M., Balis, D., Bais, A., Gerasopoulos, E., Stavrou, T., van Geffen, J., Eskes, H., and Richter, A.: Evaluation of the LOTOS-EUROS NO<sub>2</sub> simulations using ground-based measurements and S5P/TROPOMI observations over Greece, *Atmos. Chem. Phys. Discuss.* [preprint], <https://doi.org/10.5194/acp-2020-987>, in review, 2020.
- Stavrou, T., Müller, J.-F., Boersma, K. F., De Smedt, I., and van der A, R. J.: Assessing the distribution and growth rates of NO<sub>x</sub> emission sources by inverting a 10-year record of NO<sub>2</sub> satellite columns, *Geophys. Res. Lett.*, 35, L10801, <https://doi.org/10.1029/2008GL033521>, 2008.
- Timmermans, R., Eskes, H., Builtjes, P., Segers, A., Swart, D., and Schaap, M.: LOTOS-EUROS Air Quality Forecasts by Assimilation of OMI Tropospheric NO<sub>2</sub> Columns, in: *Air Pollution Modeling and its Application XXI. NATO Science for Peace and Security Series C: Environmental Security*, edited by: Steyn, D. and Trini Castelli, S., Springer, Dordrecht, the Netherlands, 2011.
- van der A, R. J., Eskes, H. J., Boersma, K. F., van Noije, T. P. C., Van Roozendaal, M., De Smedt, I., Peters, D. H. M. U., and Meijer, E. W.: Trends, seasonal variability and dominant NO<sub>x</sub> source derived from a ten year record of NO<sub>2</sub> measured from space, *J. Geophys. Res.*, 113, D04302, <https://doi.org/10.1029/2007JD009021>, 2008.
- van Geffen, J. H. G. M., Eskes, H. J., Boersma, K. F., Maasakkers J. D., and Veefkind, J. P.: TROPOMI ATBD of the total and tropospheric NO<sub>2</sub> data products, Report S5P-KNMI-L2-0005-RP, version 1.4.0, released 6 Feb. 2019, KNMI, De Bilt, the Netherlands, available at: <http://www.tropomi.eu/documents/atbd/> (last access: 8 May 2020), 2019.
- Veefkind, J. P., Aben, I., McMullen, K., Förster, H., de Vries, J., Otter, G., Class, J., Eskes, H. J., de Haan, J. F., Kleipool, Q., van Weele, Hasekamp, O., Hoogeveen, R., Landgraf, J., Snel, R., Tol, P., Ingmann, R., Voors, R., Kruizing, B., Vink, R., Visser, H., and Levelt, P. F.: TROPOMI on the ESA Sentinel-5 Precursor: A GMES mission for global observations of the atmospheric composition for climate, air quality and ozone layer applications, *Remote Sens. Environ.*, 120, 70–83, <https://doi.org/10.1016/j.rse.2011.09.027>, 2012.
- Virghileanu, M., Săvulescu, I., Mihai, B.-A., Nistor, C., and Dobre, R.: Nitrogen Dioxide (NO<sub>2</sub>) Pollution Monitoring with Sentinel-5P Satellite Imagery over Europe during the Coronavirus Pandemic Outbreak, *Remote Sens.*, 12, 3575, <https://doi.org/10.3390/rs12213575>, 2020.
- Vlemmix, T., Eskes, H. J., PETERS, A. J. M., Schaap, M., Sauter, F. J., Kelder, H., and Levelt, P. F.: MAX-DOAS tropospheric nitrogen dioxide column measurements compared with the Lotos-Euros air quality model, *Atmos. Chem. Phys.*, 15, 1313–1330, <https://doi.org/10.5194/acp-15-1313-2015>, 2015.
- Vrekoussis, M., Richter, A., Hilboll, A., Burrows, J. B., Gerasopoulos, E., Lelieveld, J., Barrie, L., Zerefos, C., and Mihalopoulos, N.: Economic Crisis Detected from Space: Air Quality observations over Athens/Greece, *Geophys. Res. Lett.*, 40, 458–463, <https://doi.org/10.1002/grl.50118>, 2013.
- World Health Organization (WHO): *Ambient air pollution: A global assessment of exposure and burden of disease*, World Health Organisation, ISBN 9789241511353, Bonn, Germany, 2016.
- Zyrichidou, I., Balis, D. S., Koukouli, M., Drosoglou, T., Bais, A., Gratsea, M., Gerasopoulos, E., Liora, N., Poupkou, A., and Giannaros, C.: Adverse results of the economic crisis: A study on the emergence of enhanced formaldehyde (HCHO) levels seen from satellites over Greek urban sites, *Atmos. Res.*, 224, 42–51, <https://doi.org/10.1016/j.atmosres.2019.03.017>, 2019.